Light & Engineering
Vol. 27, No. 5, pp. 55–62, 2019
https://doi.org/10.33383/2018-078

METHOD OF VEGETATION DETECTION USING RGB IMAGES MADE BY UNMANNED AERIAL VEHICLES ON THE BASIS OF COLOUR AND TEXTURE ANALYSIS

Michael Yu. Kataev and Maria M. Dadonova

Tomsk State University of Control Systems, Tomsk
E-mail: kataev.m@sibmail.com; mashadad@mail.ru

ABSTRACT

The article describes the capability of application of *RGB*[1] images made by digital cameras for detection of Earth surface (vegetation) types. A set of measures necessary to be taken for processing of the images made by unmanned aerial vehicles (UAV) in real-time is described. Application of analogue of vegetation index allows detecting vegetation on an *RGB* image, which increases the probability of correct detection of surface (vegetation) type. Methods of preliminary and thematic processing of images required for positive detection of surface types are considered. Texture analysis is applied for detection of vegetation type. The results of the processing of real images are provided.

Keywords: images, unmanned aerial vehicles, image processing, texture analysis, surface types

1. INTRODUCTION

Detection of types of Earth surface is an important problem for research and practice. One of the variants of solving this problem is the application of multispectral and hyperspectral data of Earth remote sensing [1, 2]. The data may be acquired using space and plane systems. The main developed methods include processing of surface images acquired in open spectral channels located in different regions of the spectrum. Preliminary knowledge of reflection spectra of Earth surface allows building methods of segmentation of Earth surface areas, therefore, to automatically categorise them. However, there is a specific aspect of such surveys related to the significant effect of the following confounders on measurements: measurement instrument, the illuminance of Earth surface, and atmosphere condition. All these factors cause imprecision of spectral properties of surveyed objects (surface types), therefore, they make it less probable to distinguish one object from another.

Application of data of spectral measurements conducted by unmanned aerial vehicles (UAV) allows increasing efficiency of detection and recognition of an object. This type of measurements is used for solving practical problems of agriculture, geology, geophysics, and Ministry of Emergency Situations [3]. For these purposes, many methods based on analysis of data acquired in specially selected combinations of spectral channels in different spectrum regions were developed. Complexity of processing of multispectral and hyperspectral [4] data is related to consideration of aspects of the process of measurement and the volume of acquired data. The acquired multidimensional image contains spatial and spectral information, where every pixel contains the vector of the spectral behaviour of a surface area consisting of subareas of different types. Before processing such data, it is necessary to take the distinctions of solar radiation transport through the atmosphere in the territory occupied (displayed) by this pixel. Variability of the acquired spectra for a particular pixel is high and depends on season and atmosphere condition.

[1] Digital model of an image

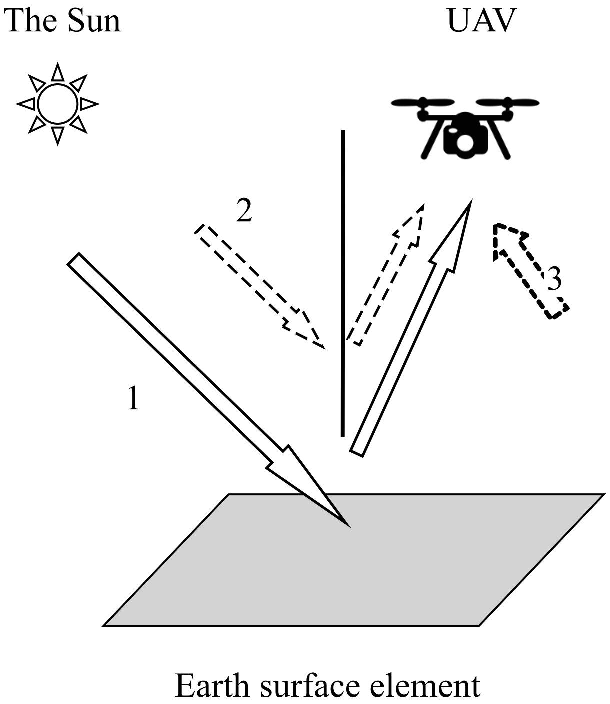

Fig. 1. Solar radiation fluxes received by optical receiver on board an UAV: 1 – radiation reflected from the surveyed area; 2 – radiation scattered in the atmosphere; 3 – diffused radiation

Digital images acquired by UAV are seldom applied for detection and recognition. This article considers the approach based on the combination of texture and colour analyses [5, 6] of acquired images for detection of vegetation on the images and recognition of its different types.

2. PROBLEM FORMULATION

A digital camera allows acquiring (measuring) images, which are possible to be processed by means of computer vision methods [7]. Then the acquired information, which most often constitutes an *RGB* image or multispectral data, is processed by means of relevant algorithms. The information on a *2D* image is a fixed radiation reflected from objects of the *3D* world. The quality of the image is determined by technical specifications of a measurement instrument (digital camera), the intensity of reflected radiation (zenith angle of the Sun and solar azimuth), type, the distance of the reflecting object, and the background (scene) [8]. Methods of computer vision allow extracting a large amount of information (colour, dimensions, form, etc.) out of the images. In the area of processing of the results of measurements acquired by means of UAV, the methods of computer vision are related to extraction of information out of the acquired data and its analysis.

A digital *RGB* image may be considered as two two-dimensional matrices with each matrix position corresponding to one pixel. For 8-bit images, the value of the magnitude measured in each pixel varies within the range of [0–255]. When designing processing methods, it is necessary to take into account that the image contains information, which is mainly determined by direct solar radiation and solar radiation reflected from different surface types. In the course of operation with images acquired by means of optic meters, it is necessary to take their radiometric characteristics, survey parameters, and atmosphere condition into account. In Fig. 1, a simplified scheme of information recording, which depends on the time of the day by an optic meter installed on the board of a UAV at a particular altitude above the Earth surface, is shown.

As it is shown in the figure, the radiation incident on the receiver is determined by reflected, scattered, and diffuse solar radiant fluxes. The solar radiation is partially absorbed by gases or scattered in the atmosphere, its part is absorbed and reflected by different types of surface. The measured data cannot be directly compared with reflection of particular surface types since there are many factors the radiation incident on the receiver depends on, such as receiver characteristics, settings of the digital camera, altitude and angle of surveying, survey conditions (solar azimuth and angle), atmosphere conditions (gas and aerosol composition of atmosphere), reflectivity of a surface. Therefore, before processing of the acquired images transforming contained data into surface reflectivity, it is necessary to conduct geometric and radiometric calibration [9].

3. CALIBRATION OF THE IMAGES MEASURED BY UAV

Combined geometric and radiometric calibration is especially necessary for comparison of data sets collected within several time periods. Naturally, receivers of the same territory register different data determined by illumination and survey conditions in different time periods. One of the differences regularly occurring in the course of real-time measurements is the change of flight altitude and angle of view, which depends on speed and direction of the wind. As digital cameras have a wide angle of view, the same area of the surface will be measured at different angles, whereas differences in time of the day when measurements are conducted and atmosphere conditions determined changes of illuminance (Fig. 2). It is especially necessary when a surface has a certain slope, which leads to changes of a measured magnitude, which depends on the angle of slope of the measured surface. Changes of UAV position depending on wind direction lead to changes of an image orientation in relation to the one acquired earlier (Fig. 2).

The radiometric correction allows correcting all measured values of radiation to the same conditions, i.e. to take the values of solar zenith and azimuth topography and illuminance (day of a year) values into account [9, 10]. Effect of the atmosphere is conditioned by aerosol scattering and absorption by gases. Usually, at a low latitude of UAV flight (100 m and less), atmospheric correction is practically not required. However, in some cases when the optical thickness of aerosol or mist may reach sufficient values, an atmospheric correction may be used [11]. Since most natural objects have anisotropic reflection characteristics, topographic effect correction is required [12].

Solar illumination geometry and terrain correction of a measured image *Im* may be presented by an expression:

$$I(i,j)=\frac{Im(i,j)\cdot\cos(Z)}{\cos(Z)\cdot\cos\big(S(i,j)\big)+\sin(Z)\times\times\sin\big(S(i,j)\big)\cdot\cos\big(Az-As(i,j)\big)}, \qquad (1)$$

where $I(i,j)$ is the corrected image, (i,j) are indexes of the current pixel of an image, Z is the zenith angle of the Sun, S is the surface angle of slope, Az is the solar azimuth, As is the azimuth of a surface related to Northern direction. The terrain parameters (As and S) may be calculated using formulas given in [13, 14].

Geometric correction of acquired images conditioned by the deviation of flight trajectory from the set one caused by the wind may be conducted using the methods described in [15, 16].

Another aspect requiring attention for each image acquired in the course of the UAV flight above the surveyed territory is a colour correction. For this purpose, we propose to use the "grey world" method [17], when it is presumed that the sum of all colours of an image gives grey colour. By calculating the average values of chromaticity in each channel, it is possible to conduct the scaling of all subsequent images as compared to the first one. This will lead to equalising of chromaticity of all measured images.

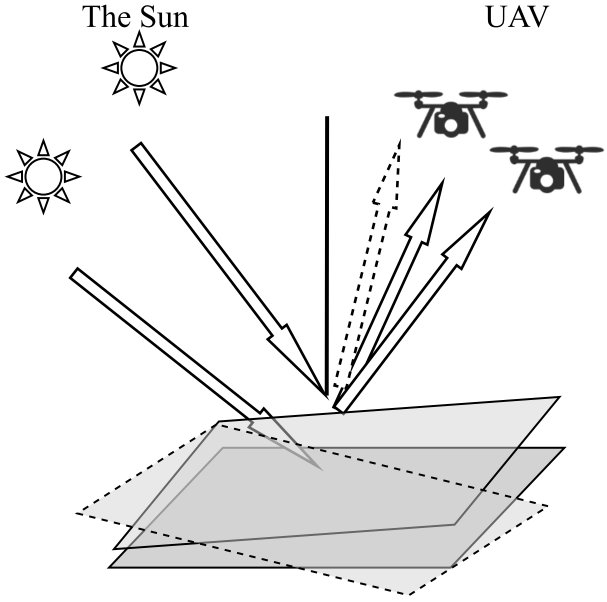

Fig. 2. Effect of measurement conditions and surface slope angle on solar radiant fluxes received by optical receiver on board an UAV

Average chromaticity for *RGB* channels may be calculated using the following formulas:

$$\langle R\rangle=\sum\sum\frac{R(i,j)}{N\cdot M};\langle G\rangle=\sum\sum\frac{G(i,j)}{N\cdot M};\quad \langle B\rangle=\sum\sum\frac{B(i,j)}{N\cdot M}, \qquad (2)$$

where R, G and B are the values of chromaticity for R, G and B channels respectively, N and M are the horizontal and vertical numbers of pixels respectively.

The value of grey colour may be calculated using the following formula:

$$Grey=\frac{w1\langle R\rangle+w2\langle G\rangle+w3\langle B\rangle}{3}, \qquad (3)$$

where $w1$, $w2$, and $w3$ are empirical coefficients (e.g. $w1$ = 0.213, $w2$ = 0.715, $w3$ = 0.072 for chromaticity analysis, $w1$ = 0.299, $w2$ = 0.587, $w3$ = 0.114 for illuminance analysis).

Then chromaticity transformation for each channel will be conducted using the following formulas:

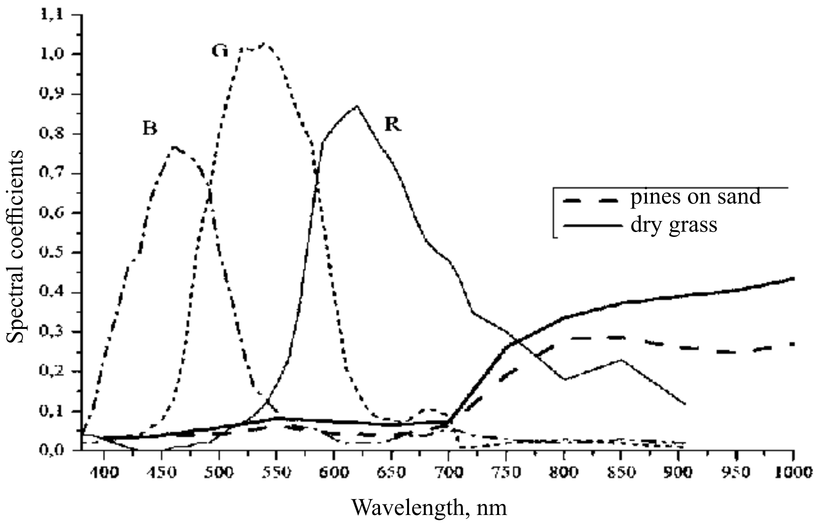

Fig. 3. Spectral response in *RGB* channels of *Canon* digital camera and spectral reflectance of vegetation

$$Rn(i,j) = \frac{R(i,j)\cdot Grey}{\langle R\rangle},\quad Gn(i,j) = \frac{G(i,j)\cdot Grey}{\langle G\rangle},\quad Bn(i,j) = \frac{B(i,j)\cdot Grey}{\langle B\rangle}, \tag{4}$$

where *Rn*, *Gn*, and *Bn* are the new values in the *R*, *G*, and *B* channels of an image respectively.

3. VEGETATION INDEXES

After preparation of the measured images, different problems of thematic processing may be solved. At the first step of processing, it is necessary to solve the problem of vegetation accentuation against the background (soil, buildings, etc.). One of the methods is related to calculation of *Colour Vegetation Index* [18], which unites radiation of two or more spectral bands reflected from the surface, which are related to *RGB* spectral coefficients of the digital camera and vegetation characteristics (Fig. 3). For calculation of vegetation characteristics from outer space, a popular one is *NDVI* (*Normalised Difference Vegetation Index*) [19] as it is calculated on the basis of green (500 nm) and near-infrared (800 nm) channels. Calculation of the difference between radiations with two values of wavelength allows to accentuate vegetation on a satellite photo. A typical digital camera installed on UAV is not equipped with a near infrared-channel, whereas the red channel includes the maximum of spectral reflectance of vegetation only partially (Fig. 3).

Nevertheless, the vegetation index *NDVI* may be calculated on the basis of the digital camera data:

$$NDVI = \frac{G-R}{G+R}\,. \tag{5}$$

Visible Vegetation Index (*VVI*) is a criterion of vegetation quantity in accordance with the following formula [20]:

$$VVI = \left[\left(1-\left|\frac{R-R_0}{R+R_0}\right|\right)\cdot\left(1-\left|\frac{G-G_0}{G+G_0}\right|\right)\times\left(1-\left|\frac{B-B_0}{B+B_0}\right|\right)\right]^{\frac{1}{w}}, \tag{6}$$

where *R, G, B* are the red, green, and blue channels of the image respectively; *Ro, Go, Bo* are the reference values of *R, G, B* channels for a particular colour scheme [21]; *w* is the weight index (the most frequently taken equal to 1).

In addition, such index as *Excess Green Index* (*ExG*) may be calculated:

$$ExG = 2G - R - B\,. \tag{7}$$

One of the popular vegetation indexes for the accentuation of vegetation on an *RGB* image is *CC* index (*canopy cover*):

$$CC = (1+L)\times\big((G-R)\times(G+R+L)\big), \tag{8}$$

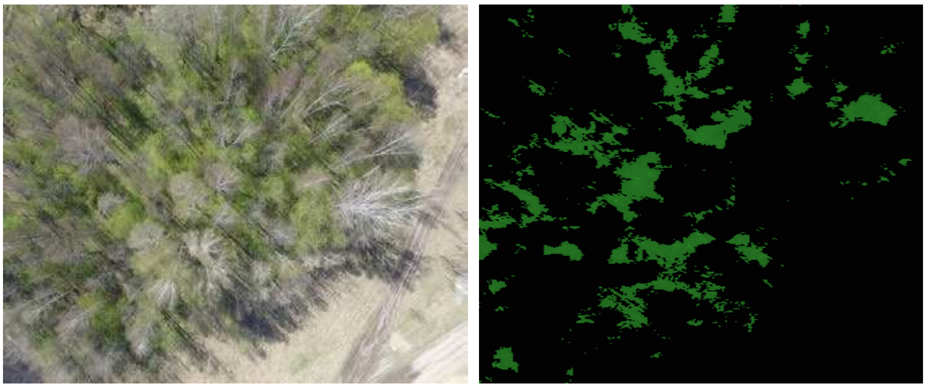

Fig. 4. Accentuation of vegetation on an image made by UAV: a – original RGB image, b – two-colour vegetation mask

where L is the soil factor equal to $L = 0$ for clean vegetation and $L = 1$ for clean soil (typically taken $L = 0.5$).

The indexes (5–8) allow accentuating areas occupied by vegetation on an image. Fig. 4 shows the result of accentuation of vegetation on an image acquired by UAV at an altitude of 15 m using filters based on the formulas (7) and (8).

4. METHOD OF VEGETATION RECOGNITION USING TEXTURE ANALYSIS

After an image acquired by means of UAV was corrected and vegetation was accentuated on it (Fig. 4b), it is possible to use the texture analysis method to determine the type of vegetation. For recognition of the vegetation type, it is necessary to process an image with a known plant and to get a template (containing only a plant without any background). Then, after conducting comparative colour and texture analysis of a new image and the template, the type of vegetation may be determined. The accentuated plant has a particular form with its area and contour possible to be measured.

For solving this problem, it is necessary to present the image in the form of shades of grey using the following expression:

$$Ig = 0.299B + 0.587G + 0.114R. \tag{9}$$

For the grey image, texture attributes are found:

– Root mean square:

$$P1 = \sum\sum \frac{\left(In(i,j)\right)^2}{N \cdot M}, \tag{10}$$

where $In(i,j) = \dfrac{Ig(i,j)}{\sum\sum Ig(i,j)}$;

– Correlation rate:

$$P2 = \sum\sum \frac{\left(In(i,j) - P1\right)}{In(i,j)}; \tag{11}$$

– Contrast (presents variations of chromaticity in different areas of the image):

$$P3 = \sum\sum (i-j)^2 \, Ig(i,j); \tag{12}$$

– Discrepancy:

$$P4 = \sum\sum |i-j| \, Ig(i,j); \tag{13}$$

– Homogeny (relatively low values of this parameter witness low difference between data):

$$P5 = \sum\sum \frac{Ig(i,j)}{\left(1-(i-j)^2\right)}, \text{ or} \tag{14}$$

$$P9 = \sum\sum \frac{Ig(i,j)}{\left(1-|i-j|\right)}; \tag{15}$$

– Entropy (value of irreversible energy dissipation):

$$P6 = \sum\sum Ig(i,j) \cdot \lg\left(Ig(i,j)\right); \tag{16}$$

– Maximum (maximum value of pixel intensity (i,j):

$$P7 = max\left(Ig(i,j)\right); \tag{17}$$

Fig. 5. Cabbage image template

– Energy (characterises length and curvedness of contour):

$$P8 = \sum\sum Ig(i,j)^2. \tag{18}$$

Then, after calculating texture attributes for the template of the required object and randomly taken areas of the image using formulas (10)–(18), the area may be categorised as an object by means of comparison. Comparison is made by calculating an approximation of the values of texture attributes with consideration of an operator:

$$C = \sum \frac{Ps(i) - P(i)}{Ps(i)}, \tag{19}$$

where Ps, P are the texture attributes for the template and the area of the image.

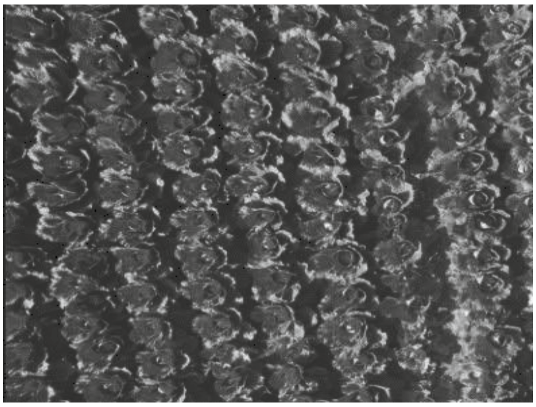

a)

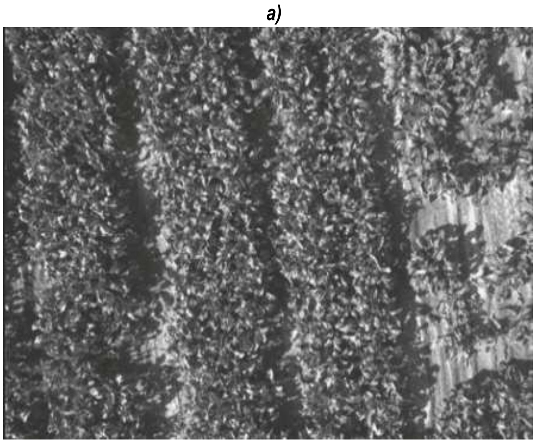

b)

Fig. 6. Test images of field areas with: a – cabbage, b – beet crops

5. RESULTS OF NUMERICAL EXPERIMENTS

As an example of the method proposed by us, the results of surveying of a field with cabbage and beet crops were taken. In Fig. 5, the template of cabbage image is shown, using it, all the described corrections were conducted and texture coefficients were calculated, the results are listed in Table 1.

Fig. 6 shows test images of the field areas with cabbage (6a) and beet (6b) crops.

Then the images were processed in order to divide them into blocks containing separate homogeneous areas for which, using formulas (10)–(18), texture attributes *P1–P9* were calculated and compared with the template attributes using formula (19). As a result, the average percentage of correct guessing for the image 6a with the criterion C > 0.9 was equal to 88 %, and after comparing the template with image 6b, it was equal to 5 %. Part of the images with open soil was not recognised.

6. CONCLUSION

Technologies of monitoring by means of unmanned aerial vehicles are gradually being introduced into many spheres of research and practice. Technological problems of UAV development, routing, and measurements have already been transferred to ordinary routine mode. However, there is still a lack of processing software and especially software for analysis of the information acquired by means of UAV, and only some problems are solved. One of the problems, which is the most often solved by means of multispectral and hyperspectral equipment, is the classification of surface types. Such type of measurements allows solving problems of classification with high precision but is rather expensive and demanding in terms of measurement

Table 1. Texture Coefficients for the Cabbage Image Template (Fig. 5)

Texture coefficient	Average value	Dispersion
P1	$2.592 \cdot 10^{-5}$	$6.528 \cdot 10^{-7}$
P2	$2.782 \cdot 10^{4}$	$9.342 \cdot 10^{2}$
P3	$2.857 \cdot 10^{5}$	$5.191 \cdot 10^{3}$
P4	$1.419 \cdot 10^{2}$	1.262
P5	$8.883 \cdot 10^{-4}$	$6.945 \cdot 10^{-5}$
P6	6.322	$7.962 \cdot 10^{-2}$
P7	$1.811 \cdot 10^{-3}$	$1.449 \cdot 10^{-4}$
P8	$2.101 \cdot 10^{-3}$	$1.521 \cdot 10^{-4}$
P9	$5.057 \cdot 10^{-2}$	$1.320 \cdot 10^{-3}$

conditions. A simpler method proposed in this article is based on the application of a simple *RGB* digital camera. As atmospheric conditions of acquiring digital images constantly change, for equalisation of conditions of all images, geometric and radiometric correction is used. For recognition of surface types (several types of vegetation are considered in the article), we use textural analysis. The results given in the work confirm high precision of recognition of vegetation types on the basis of *RGB* images acquired by means of UAV. It should be noted that the texture analysis algorithm applied in this work is a rather simple one, and if it is used in more complex modifications, it should allow more precision type recognition for acquiring essential values of surface (vegetation in particular).

ACKNOWLEDGEMENT

The study was conducted as part of the national order of the Ministry of Education and Science of the Russian Federation, Project No. 8.8184.2017/8.9 “Methodology of Development of Energy-Generating and Energy-Transforming Systems for Onshore and Onboard Units of Onshore, Space and Underwater Facilities” and a youth project under the UMNIK programme.

REFERENCES

1. Kashkin V.B. Distantsionnoe zondirovanie Zemli iz kosmosa. TSifrovaia obrabotka izobrazhenii: ucheb. posobie [Remote Sensing of Earth from Outer Space. Digital Processing of Images: study guide] // Logos, Moscow, 2001, 264 p.

2. Chandra A.M., Gosh S.K. Distantsionnoe zondirovanie i geograficheskie informatsionnye sistemy [Remote Sensing and Geographic Information Systems] // Tekhnosphera, Moscow, 2008, 312 p.

3. Fetisov V.S. Bespilotnaia aviatsiia: terminologiia klassifikatsiia sovremennoe sostoianie [Unmanned Aviation: Terminology, Classification, Contemporary Development] // Photon, Ufa, 2014, 217 p.

4. Starovoytov V.V., Golub Yu.I. Tsifrovye izobrazheniia ot polucheniia do obrabotki [Digital Images: from Acquiring to Processing] // OIPI NAN, Minsk, 2014, 202 p.

5. Yanshin V.V., Kalinin G.A. Obrabotka izobrazhenii na iazyke Si dlia IBM PC: Algoritmy i programmy [Processing Images on C for IBM PC: Algorithms and Programmes] // Mir, Moscow, 1994, 240 p.

6. Pratt W. Tsifrovaia obrabotka izobrazhenii [Digital Processing of Images] // Mir, Moscow, 1982, Vol. 1–2, 1104 p.

7. Shapiro L., Stockman J. Kompiuternoe zrenie [Computer Vision] // Binom, Laboratoria Znany, Moscow, 2006, 752 p.

8. Visilter Yu.V., Zheltov S. Yu., Bondarenko A.V., Ososkov M.V., Morzhin A.V. Obrabotka i analiz izobrazhenii v zadachakh mashinnogo zreniia [Processing and Analysis of Images in Computer Vision Problems] // Fizmatkniga, Moscow, 2010, 672 p.

9. Hruska R., Mitchell J., Anderson M., Glenn N.F. Radiometric and geometric analysis of hyperspectral imagery acquired from an unmanned aerial vehicle // Remote Sens, 2012, No. 4, pp. 2736–2752.

10. Shepherd J.D., Dymond J.R. Correcting satellite imagery for the variance of reflectance and illumination with topography // Int. J. Remote Sens, 2003, Vol. 24, pp. 3503–3514.

11. Colomina I., Molina P. Unmanned aerial systems for photogrammetry and remote sensing: A review // ISPRS J. Photogramm. Remote Sens, 2014, Vol. 92, p. 79–97.

12. Huang W., Zhang L., Li P.-X. A Topographic Correction Approach for Radiation of RS Images by Using Spatial Context Information // Acta Geodaetica Et Cartographica Sinica, 2006, Vol. 35, No. 8, pp. 286–290.

13. Dybayah R., Rich P. Topographic solar radiation models for GIS // International Journal of Geographical Information Systems, 1995, No. 9, pp. 405–419.

14. Bolstad P.V., Smith J.L. An Evaluation of DEM Accuracy: Elevation, Slope Aspects // Photographic Engineering and Remote Sensing, 1994, Vol. 60, No. 11, pp. 1327–1332.

15. Toutin T. Geometric Processing of Remote Sensing Images: Models, Algorithms and Methods // International Journal of Remote Sensing, 2004, Vol. 25, No. 10, pp. 1893–1924.

16. Kim J., Kim T. Fast and robust geometric correction for mosaicking UAV images with narrow overlaps // International Journal of Remote Sensing, 2017, Vol. 38, No. 8–10, pp. 2557–2576.

17. Reinhard E., Adhikhmin M., Gooch B., Shirley P. Color transfer between images // IEEE Computer graphics and applications, 2001, Vol. 21, No. 5, pp. 34–41.

18. Meyer G.E., Neto C.J. Verification of color vegetation indices for automated crop imaging applications // Computers and electronics in agriculture, 2008, Vol. 63, No. 2, pp. 282–293.

19. Bannari A., Morin D., Bonn F., Huete A.R. A review of vegetation indices // Remote Sensing Reviews, 1995, Vol. 13, pp. 95–120.

20. URL: http://phl.upr.edu/projects/visible-vegetation-index-vvi.

21. URL: https://colorscheme.ru.

Michael Y. Kataev,
Prof., Dr. of Tech. Sciences. Graduated from Tomsk State University with specialty Optic Engineering Researcher (1984). Professor of the Automated Control Systems (ACS) department of the Tomsk State University of Control Systems and Radioelectronics (TUSUR), Professor of Yurga Technological Institute (branch) of the National Research Tomsk Polytechnic University. Head researcher of the TUSUR Centre of Space Monitoring of Earth

Maria M. Dadonova,
Master Degree Student of ACS department of TUSUR University